Thin Solid Films 605 (2016) 143–148

Contents lists available at ScienceDirect

Thin Solid Films

journal homepage: www.elsevier.com/locate/tsf

Effects of concentration of reduced graphene oxide on properties of sol–gel prepared Al-doped zinc oxide thin films

Ching-Tian Chou, Fang-Hsing Wang *, Wei-Chun Chen

Department of Electrical Engineering and Graduate Institute of Optoelectronic Engineering, National Chung Hsing University, No. 250, Kuo-kuang Rd., Taichung 40227, Taiwan, ROC

ARTICLE INFO

Article history:
Received 7 May 2015
Received in revised form 13 November 2015
Accepted 13 November 2015
Available online 14 November 2015

Keywords:
Aluminum-doped zinc oxide
Reduced graphene oxide
Transparent conductive oxide
Sol–gel

ABSTRACT

Reduced-graphene-oxide-incorporated aluminum-doped zinc oxide (AZO:rGO) composite thin films were synthesized on glass substrates by using the sol–gel method. The effect of the rGO concentration (0–3 wt%) on structural, electrical, and optical properties of the composite film was investigated by X-ray diffraction, scanning electron microscopy, atomic force microscopy, Hall-effect measurement, and ultraviolet–visible spectrometry. All of the composite films showed a typical hexagonal wurtzite structure, and the films incorporated with 1 wt% rGO showed the highest (0 0 2) peak intensity. The sheet resistance of the films was effectively reduced by a factor of more than two as the rGO ratio increased from 0 to 1 wt%. However, the sheet resistance increased with a further increase in the rGO ratio. The optical transmittance of the composite film monotonically decreased with increasing the rGO ratio from 0 to 3 wt%. The average optical transmittance (400–700 nm) of the AZO:rGO thin film within 1 wt% rGO was above 81%.

1. Introduction

A transparent conductive oxide (TCO) thin film is a critical component of many optoelectronic devices, such as liquid crystal displays, touch panels, photovoltaic solar cells, and organic light-emitting diodes [1–3]. Indium tin oxide (ITO) films have been used as TCOs because of their low electrical resistivity and high transparency to visible light [4]; however, they have several disadvantages: they are (1) toxic, (2) costly, and (3) inflexible. Al-doped ZnO (AZO) [5,6] thin films are currently under intense investigation and development because of their strong potential for use in optoelectronic applications. Magnetron sputtering has already been shown to produce AZO thin films with a comparable resistivity to that of tin-doped indium oxide (ITO) thin films. However, it needs high vacuum atmosphere and its deposition rate is relatively slow, leading to the increase of the production cost. The sol–gel technique is economically efficient in preparing large area AZO thin films. However, the resistivity of the sol–gel AZO films is generally in the order of 10^{-2}–10^{-3} Ω-cm, which is higher than that of the sputtered ones [7]. How to improve the electrical conductivity of sol–gel AZO films is worthy to study.

Carbon materials, particularly carbon nanotubes (CNTs) and graphene, have favorable and stable characteristics that render them suitable for use in semiconductor device applications [8,9]. CNTs, discovered in 1991 by Iijima [10], are one-dimensional materials; the optical transmittance of CNT thin films decreases appreciably with a decrease in sheet resistance, and therefore, CNTs are not an appropriate TCO material [11]. Graphene, a two-dimensional single layer of sp^2-bonded carbon atoms, has attracted considerable research interest because of its excellent electrical conductivity, thermal, and mechanical properties [12]. There are several methods for synthesizing graphene: (1) chemical methods such as chemical vapor deposition (CVD) [13], (2) mechanical exfoliation [14], and (3) reduction of graphene oxide [15,16]. Graphene thin films prepared using CVD show excellent performance compared with those prepared using other methods. Among these techniques, a solution based on a coating technique [17] and vacuum filtration [18] has been used for transparent reduced graphene oxide (rGO) thin film fabrication. However, rGO thin films fabricated using a solution-based method show high sheet resistance [19] for TCO applications. To enhance the electrical conductance and optical transmittance of rGO thin films, oxygen functional groups [20] were used on rGO thin films; the developed films showed optoelectronic properties, a resistivity of 1.1 kΩ/□, and a transmittance of 89% at a wavelength of 550 nm. In addition, Bu [21] proposed AZO:rGO composite thin films and investigated the effect of the annealing temperature on their optoelectronic properties. Gyorgy et al. studied the surface morphology, structure, and photoactive properties of ZnO:GO (where GO is the abbreviation for graphene oxide) composite thin films [22]. Besides, no other study has been conducted on AZO:rGO composite thin films.

In this study, we fabricated AZO:rGO thin films by the sol–gel method for transparent conducting film applications. Effects of rGO concentration on structural, electrical, and optical properties of the AZO:rGO films were investigated. The developed optimal AZO:rGO film exhibited an improved electrical property and an acceptable optical transmittance as compared with that of the AZO film without rGO.

* Corresponding author.
E-mail address: fansen@dragon.nchu.edu.tw (F.-H. Wang).

http://dx.doi.org/10.1016/j.tsf.2015.11.033
0040-6090/

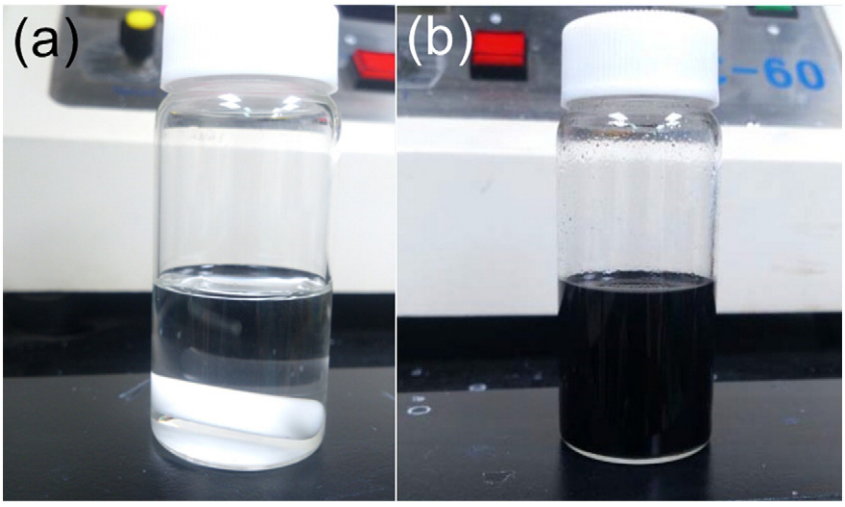

Fig 1. Photographs of the Sol–gel AZO solution before and after rGO incorporation.

2. Experiment

An AZO solution was prepared by mixing 3.2922 g of $Zn(CH_3COOH)_2 \cdot 2H_2O$ (98%) powder and 34 mg of $AlCl_3 \cdot 6H_2O$ (97%) in a 2-methoxyethanol (99%) and ethanolamine (98%) solution. The AZO solution was stirred at 60 °C for 2 h to obtain a transparent colorless and homogeneous solution. The Al content in the mixed solution was 1.0 at%.

Graphene oxide was prepared using Hummers method [23]. An amount of 0.5 g of natural graphite flakes (Merck) was mixed with 22 mL of H_2SO_4. Subsequently, 1.5 g of $KMnO_4$ was added to the acid solution and the solution was stirred at 25 °C for 30 min. Thereafter, 23 mL of deionized water was added to the composite solution slowly, and the solution was stirred at 90 °C. The color of the solution then became brown. An hour later, 5% H_2O_2 was added and rinsed with methanol. After 24 h, the matured solution was repeatedly filtered and heated at 60 °C for 24 h to obtain GO solids. To obtain rGO, 0.1 g of the GO solids was mixed with 100 mL of deionized water and sonicated for 2 h. Subsequently, 20 μL of hydrazine was added to the solution, and the solution was stirred at 95 °C for 3 h. Finally, the solution was repeatedly filtered and dried at 60 °C for 24 h. Different amounts of rGO were dissolved in the AZO solution, and the mixed solution were ultrasonically agitated for 2 h. Fig. 1(a) and 1(b) shows the obtained homogeneous solutions before and after rGO incorporation. These solutions were prepared for subsequent spin-coating.

The glass substrates (Corning 1737) were cleaned by ethanol, acetone, and deionized water and then dried in nitrogen. First, the substrates were pre-rotated with 1000 rpm and 3000 rpm for 10 s each in a spin coater. Then the AZO:rGO composite solution was dribbled on the substrate, after which the substrate was rotated with 1000 rpm

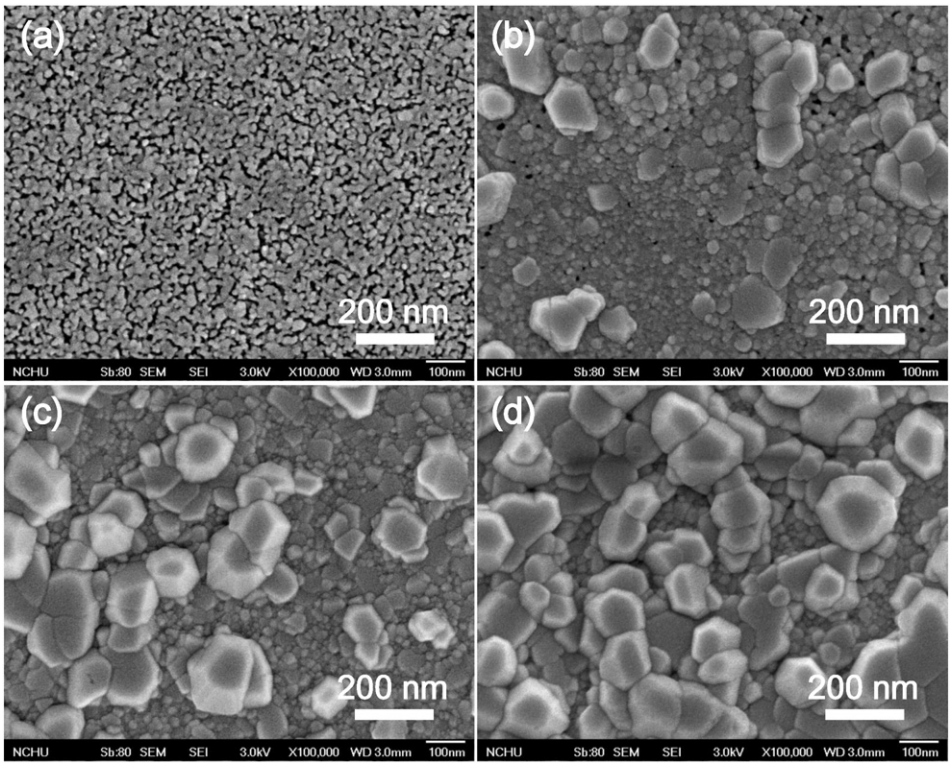

Fig. 2. Plan-view SEM images of the AZO:rGO thin films with different rGO ratios of (a) 0.0 wt%, (b) 1.0 wt%, (c) 1.5 wt%, and (d) 3.0 wt%.

and 3000 rpm for 10 s and 30 s, respectively. The substrate was then baked at 350 °C for 10 min to remove organic residuals. These spin-coating steps were repeated for 6 times to keep the thin film thickness of roughly 250 nm. These thin films were finally annealed in an environment of Ar and H_2 at 500 °C for 1 h. The structural properties of thin films were investigated by X-ray diffraction (XRD) (PANalytical, 18 kW rotating anode X-ray generator, Japan) with Cu-Kα radiation (λ = 0.154056 nm) in θ–2θ scan mode and field emission scanning electron microscopy (FE-SEM, 3.0 kV) (JEOL JSM-6700F, Japan). Surface roughness of thin films was observed by an atomic force microscope (AFM) (Veeco D3100) with a Nanoscope IV controller operated at tapping mode. The electrical properties were measured by four point probe (Napson, RT-70/RG-5, Japan) and Hall-effect measurement (Ecopia, HMS-3000) using the Van der Pauw method. The optical properties were measured by a UV–VIS spectrometer (JASCO, V-570, Japan).

3. Results and discussion

Fig. 2 shows plan-view SEM images of AZO:rGO thin films on glass substrates as a function of the rGO ratio. All of the films appeared to have been coated with rGO flakes, which had diameters ranging from 30 to 150 nm. The diameters of the rGO flakes increased with the rGO ratio, and their shape changed from small irregular shapes to large hexagon-like shapes. Fig. 3 shows cross section SEM images of AZO:rGO thin films with different rGO ratios. The average thickness of the thin films was 250 ± 10 nm.

To explore the composition of the composite films, energy dispersive X-ray spectroscopy analysis of AZO:rGO thin films with different rGO ratios was performed. Table 1 lists the element ratios in AZO:rGO films with rGO ratios of 0.0 wt% and 1.0 wt%. The amounts of C and O on the film surface increased with the amount of rGO. This result is consistent with the findings in Fig. 2. The reduced Zn content in the 1.0 wt%-rGO film is attributable to rGO flakes covering the film surface. The detected Al concentration does not obviously change and is around 7–8 at%.

Table 1
Element analysis of the AZO:rGO films from the EDS analysis.

	Weight%		Atomic%	
Element	0.0 wt%	1.0 wt%	0.0 wt%	1.0 wt%
C	6.28	10.59	13.84	19.56
O	35.21	46.58	38.08	48.64
Al	7.39	11.58	7.39	7.89
Zn	51.12	31.25	40.69	23.91
Totals	100.00	100.00	100.00	100.00

Fig. 4 shows atomic force microscopy images of AZO:rGO thin films with different rGO ratios. The roughness values of the thin films were 2.05, 10.08, 13.81, and 42 nm for rGO ratios of 0, 1.0, 1.5, and 3.0 wt%, respectively. The surface roughness increased with the rGO content because the size of the rGO flakes increased with the rGO content, as shown in the scanning electron microscopy images.

Fig. 5 shows XRD patterns of AZO:rGO thin films with different rGO ratios. All films showed a (0 0 2) peak at $2\theta \approx 34°$, indicating that the AZO:rGO thin films prepared using the sol–gel method had a hexagonal wurtzite structure and favorable *c*-axis orientation perpendicular to the substrate. The (0 0 2) peak intensity increased as the rGO ratio increased from 0 wt% to 1 wt%; however, the intensity decreased with an increase in the rGO ratio beyond 1.5 wt%.The carbon doping effect on ZnO has been intensively investigated for potential applications over the past several years [24–28]. Carbon can occupy either Zn (C_{Zn}) or O (C_O) sites during the doping process, depending on the annealing conditions. In the current investigation, while the AZO:rGO films were annealed in an Ar + H_2 atmosphere, carbon atoms might have occupied Zn^{2+} vacancies to form C_{Zn} defects [26–28].

Table 2 shows the structural parameters of the AZO:rGO films shown in Fig. 4. The crystalline plane distance (d) was estimated using the Bragg formula: $\lambda = 2d\sin\theta$, where λ is the X-ray wavelength (0.154056 nm) and θ is the diffraction angle of the (0 0 2) peak. The lattice constant, *c*, is equal to 2*d* for the (0 0 2) diffraction peak. The strain (ε) of the films in the direction of the *c*-axis is given by the equation $\varepsilon =$

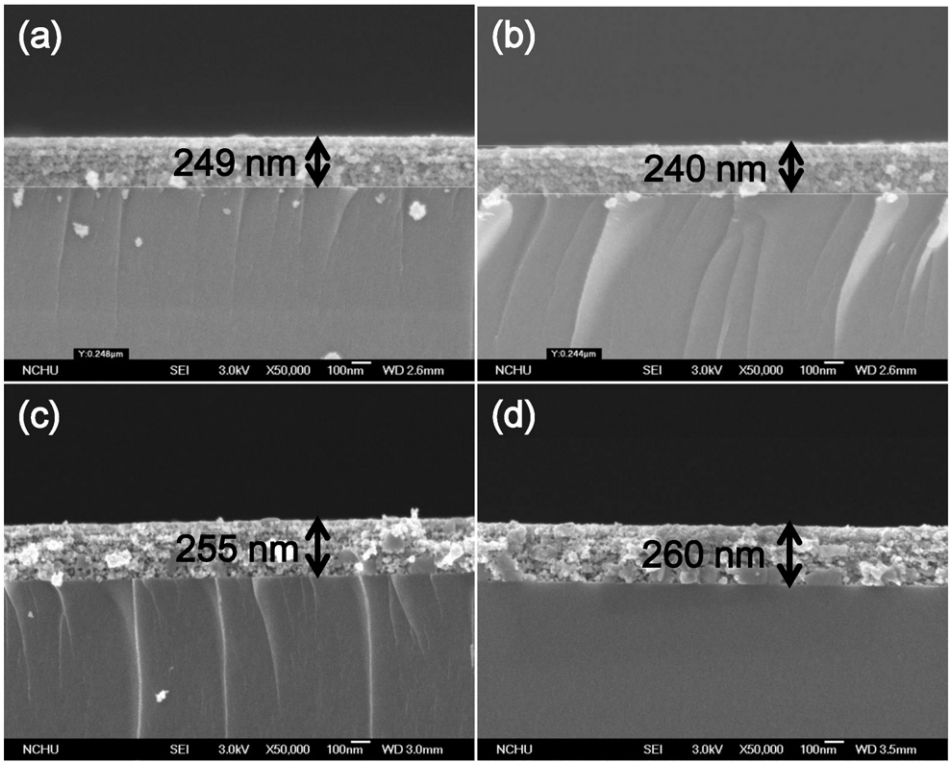

Fig. 3. Cross-section SEM images of the AZO:rGO thin films with different rGO ratios of (a) 0.0 wt%, (b) 1.0 wt%, (c) 1.5 wt%, and (d) 3.0 wt%.

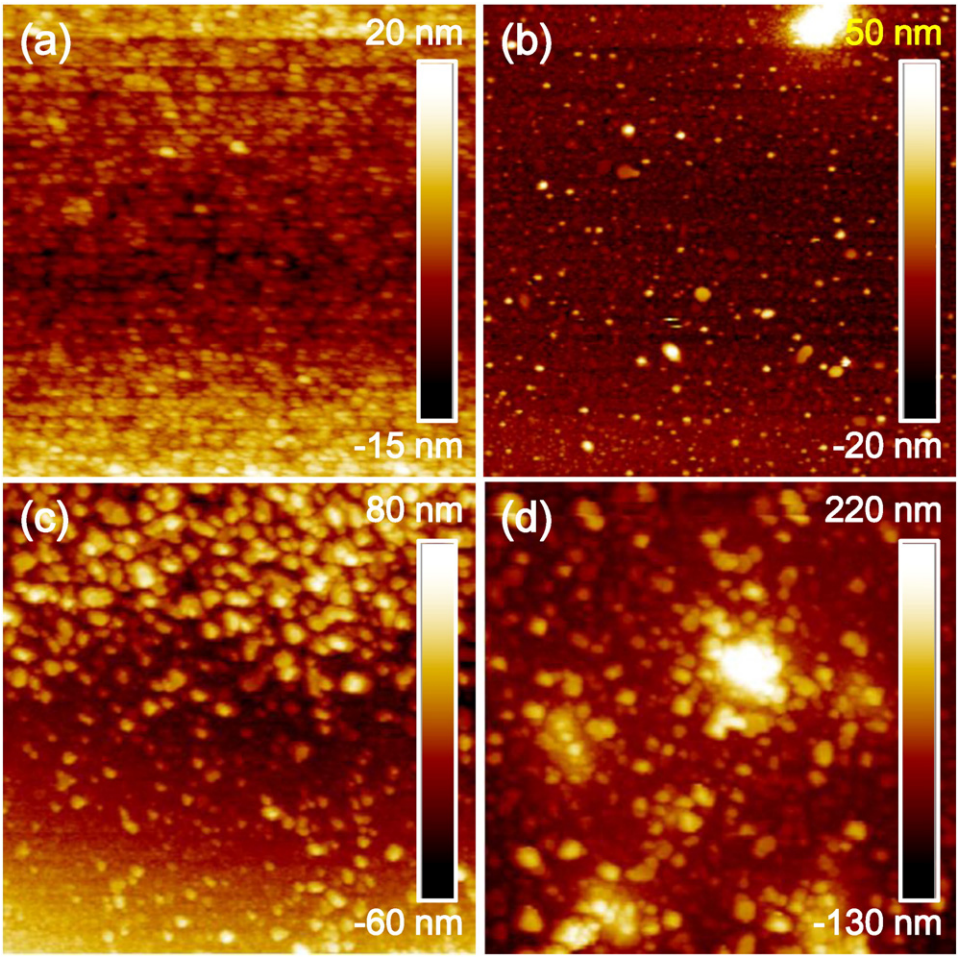

Fig. 4. AFM image of the AZO:rGO thin films with different rGO ratios of (a) 0.0 wt%, (b) 1.0 wt%, (c) 1.5 wt%, and (d) 3.0 wt%.

$[(c_{film} - c_{bulk})/c_{bulk}]$, where c_{bulk} is the unstrained lattice parameter measured from bulk ZnO [29]. The stress in the films increased with the rGO ratio, and the increase was caused by the rGO flakes embedded in the films. The increase in stress could have led to cracks appearing on the surface. Fig. 6 shows the relationship between the sheet resistance and the XRD peak intensity. Clearly, a higher peak intensity resulted in a lower sheet resistance, implying that the crystallinity was correlated with the sheet resistance.

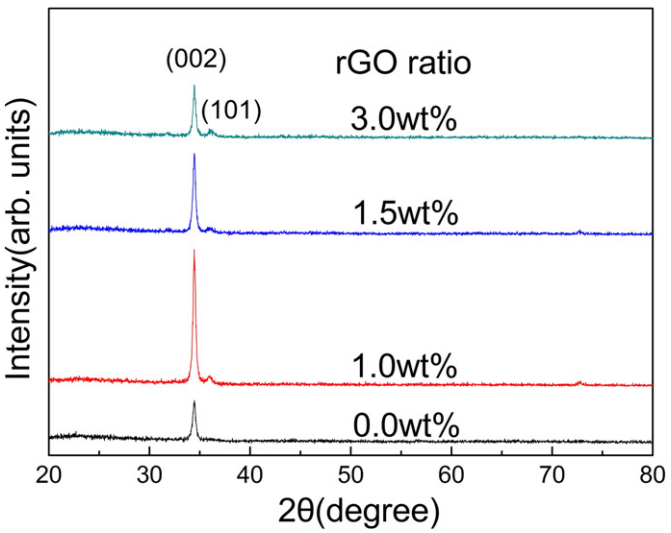

Fig. 5. XRD patterns of the AZO:rGO thin films with different rGO ratios.

Fig. 7 shows the optical transmittance of AZO:rGO thin films with different rGO ratios. The average optical transmittance of the AZO:rGO film without rGO was 92.8% in visible wavelength range (400–700 nm). When the rGO ratio was 0.5 wt%, the average optical transmittance decreased to 88.1%. Comparatively, the thin film with an rGO ratio of 3.0 wt% showed a reduced average transmittance of 50.9%. Generally, the average optical transmittance decreased with an increase in the rGO ratio because a higher rGO ratio resulted in a larger amount of rGO flakes on the surface, and an increase in the amount of rGO flakes enhanced light absorption, leading to reduced transparency [30]. The long-term stability of the optical transmittance was also investigated. Fig. 8 shows the transmittances of the composite films without and with 0.5 wt% rGO after around 800 days as the samples were kept in a small plastic case in the atmosphere. It was found that their average transmittances in the wavelength of 400–700 nm did not significantly vary regardless of rGO content after the long-term test. This result indicated the developed AZO:rGO films possess superior optical stability.

Table 2
Structural parameters of the AZO:rGO films calculated from the XRD patterns.

rGO Concentration (wt%)	2θ(°)	FWHM (°)	Grain size (nm)	d (nm)	c (nm)	Stress (GPa)
0.0	34.5	0.326	25.51	0.2597	0.5195	−0.019
1.0	34.48	0.324	25.67	0.2599	0.5198	−0.582
1.5	34.48	0.313	26.57	0.2599	0.5198	−0.594
3.0	34.5	0.297	28.01	0.2597	0.5195	−1.145

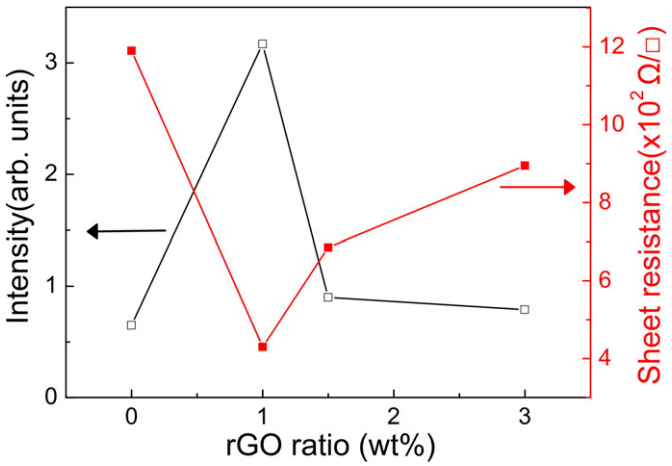

Fig. 6. Relationship between the sheet resistance and the XRD (0 0 2) peak intensity.

Fig. 9(a) and 9(b) shows the sheet resistance, carrier concentration, and Hall mobility of AZO:rGO thin films as a function of the rGO ratio. The rGO sheet resistance could be effectively reduced by increasing the rGO ratio to a high value. The sheet resistance of AZO:rGO thin films with 1 wt% rGO decreased by a factor greater than two compared with that in the absence of rGO; however, for rGO ratios above 1 wt%, the sheet resistance increased with the rGO ratio. The Hall mobility and carrier concentration increased from 9.1 to 15.1 $cm^2/V \cdot s$ and from 2.41×10^{19} to 8.27×10^{19} cm^{-3}, respectively, for an increase in the rGO ratio from 0 to 1.0 wt%. The lowest sheet resistance was 430 Ω/□. The carrier concentration and Hall mobility increased with the rGO concentration and reached the maximum for the rGO concentration of 1.0 wt%. The increase in the Hall mobility with the rGO ratio was due to the enhanced crystallinity of the films. A decrease in the carrier concentration for rGO ratios above 1.0 wt% may be ascribed to the reduced crystallinity of the films, as indicated by the XRD diffraction pattern in Fig. 4. The increase in the Hall mobility of AZO:rGO films was because of the combined effect of an increase in the grain size and a decrease in the sheet resistance, both of which enhanced the crystallinity [31].

The time-dependent resistivity of AZO:rGO thin films with different rGO ratios is shown in Fig. 10. The possibility of the film sheet resistance increasing with time may be due to the adsorption of oxygen: the film surface absorbs oxygen from the air, leading to a decrease in the free

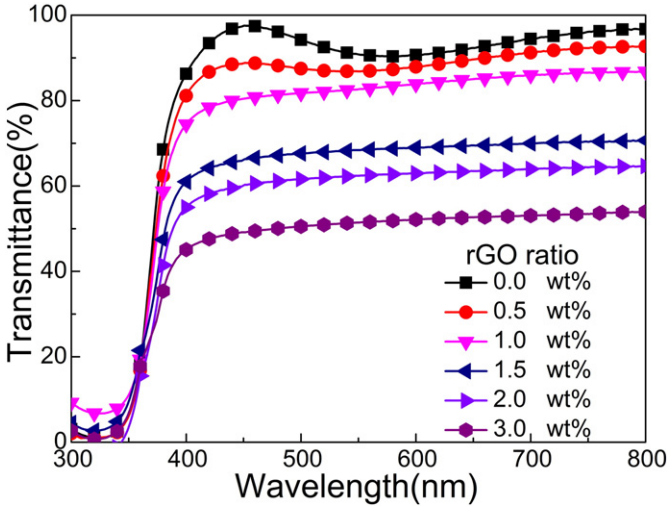

Fig. 7. Optical transmittance of the AZO:rGO thin films with different rGO ratios.

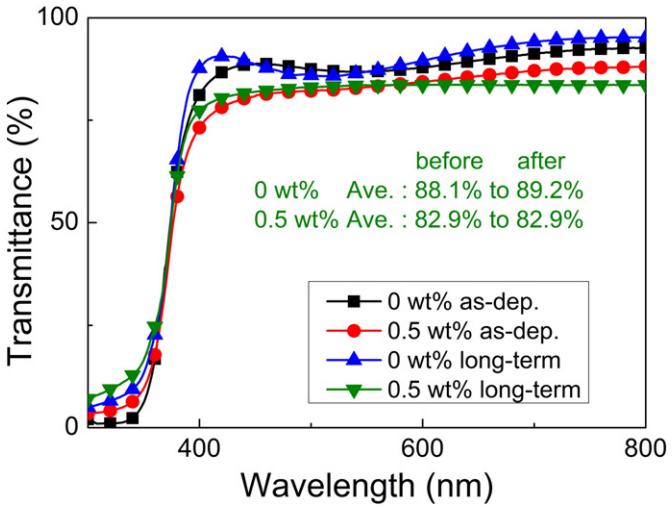

Fig. 8. Optical transmittance of the AZO:rGO thin films before and after long-term stability test.

electron and carrier concentrations [32]. However, after eight days, the sheet resistance did not change noticeably because oxygen adsorption became saturated.

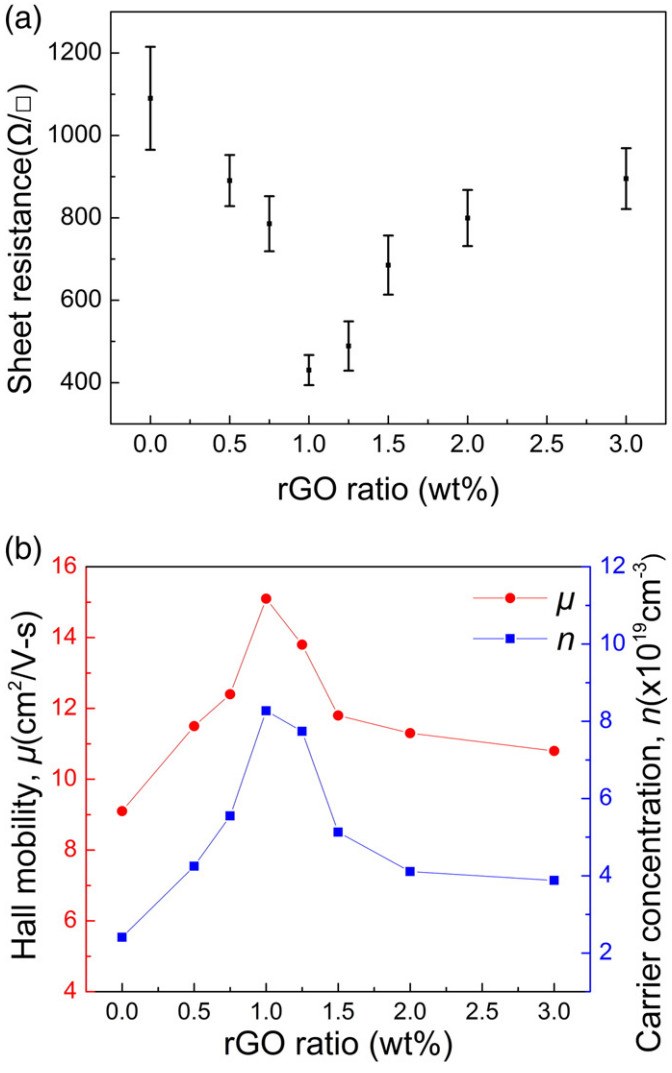

Fig. 9. (a) Sheet resistance and (b) Hall mobility and carrier concentration of the AZO:rGO thin films with different rGO ratios.

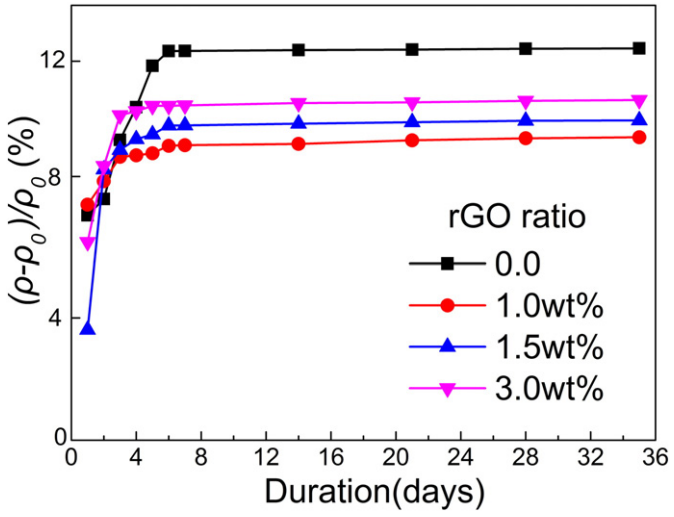

Fig. 10. The electrical stability of the AZO:rGO thin films with different rGO ratios.

4. Conclusions

Sol–gel method was used to fabricate low cost transparent conducting AZO:rGO thin films. The AZO:rGO films with different ratios were spin coating onto the glass substrates and annealing at 500 °C. The XRD pattern showed the AZO:rGO films had a hexagonal wurtzite structure and a good c-axis orientation perpendicular to the substrate. The AZO:rGO films obtained possessed remarkable properties: the sheet resistant was 430 Ω/□ and the transparency was 81% at a typical wavelength of 400–700 nm. The developed AZO:rGO thin films have potential for future optoelectronic applications.

Acknowledgements

The authors would like to thank Ministry of Science and Technology, Taiwan under the Grant MOST 103-2221-E-005-040-MY2 for financial support.

References

[1] T. Minami, T. Miyata, Present status and future prospects for development of non- or reduced-indium transparent conducting oxide thin films, Thin Solid Films 517 (2008) 1474–1477.
[2] A.V. Moholkar, S.M. Pawar, K.Y. Rajpure, V. Ganesan, C.H. Bhosale, Effect of precursor concentration on the properties of ITO thin films, J. Alloy. Compd. 464 (2008) 387–392.
[3] Y. Zhang, L. Wu, H. Li, J. Xu, L. Han, B. Wang, Z. Tuo, E. Xie, Influence of Fe doping on the optical property of ZnO films, J. Alloy. Compd. 473 (2009) 319–322.
[4] J. Hu, R.G. Gordon, Textured aluminum-doped zinc oxide thin films from atmospheric pressure chemical-vapor deposition, Jpn. J. Appl. Phys. 71 (1992) 880–890.
[5] M. Mazilu, N. Tigau, V. Musat, Optical properties of undoped and Al-doped ZnO nanostructures grown from aqueous solution on glass substrate, Opt. Mater. 1833–1838 (2012).
[6] F.H. Wang, H.P. Chang, C.C. Tseng, C.C. Huang, Effects of H_2 plasma treatment on properties of ZnO:Al thin films prepared by RF magnetron sputtering, Surf. Coat. Technol. 205 (2011) 5269–5277.
[7] K.M. Lin, H.C. Chen, Y.Y. Chen, K.Y. Chou, Influences of preferred orientation growth on electrical properties of ZnO:Al films by sol–gel method, J. Sol–Gel Sci. Technol. 55 (2010) 369–376.
[8] S.H. Kim, Y. Yu, Y.Z. Li, T. Xu, J.F. Zhi, A hybrid reduction procedure for preparing flexible transparent graphene films with improved electrical properties, J. Mater. Chem. 22 (2012) 18306–18313.
[9] I. Khrapach, F. Withers, T.H. Boiton, D.K. Polyushkin, W.L. Barner, S. Russo, M.F. Craciun, Novel highly conductive and transparent graphene-based conductors, Adv. Mater. 24 (2012) 2844–2849.
[10] S. Iijima, Helical microtubules of graphitic carbon, Nature 354 (1991) 56–58.
[11] B.T. Liu, C.H. Hsu, W.H. Wang, A comparative study on preparation of conductive and transparent carbon nanotube thin films, J. Taiwan Inst. Chem. E 43 (2012) 147–152.
[12] J. Kang, H. Kim, K.S. Kim, S.K. Lee, S. Bae, J.H. Ahn, Y.J. Kim, J.B. Choi, B.H. Hong, High-performance graphene-based transparent flexible heaters, Nano Lett. 5154–5158 (2011).
[13] S. Bae, H. Kim, Y. Lee, X. Xu, J.S. Park, Y. Zheng, J. Balakrishnan, T. Lei, H.R. Kim, Y.I. Song, Y.J. Kim, K.S. Kim, B. Ozyilmaz, J.H. Ahn, B.H. Hong, S. Iijima, Roll-to-roll production of 30-inch graphene films for transparent electrodes, Nat. Nanotechnol. 5 (2010) 574–578.
[14] A.K. Geim, K.S. Novoselov, The rise of grapheme, Nat. Mater. 6 (2007) 183–191.
[15] Y. Zhu, S. Murali, W. Cai, X. Li, J.W. Sak, J.R. Potts, R.S. Ruoff, Graphene and graphene oxide: synthesis, properties, and applications, Adv. Met. 22 (2010) 3906–3924.
[16] D.S. Hecht, L. Hu, G. Irvin, Emerging transparent electrodes based on thin films of carbon nanotubes, graphene, and metallic nanostructures, Adv. Mater. 23 (2011) 1482–1513.
[17] V.C. Tung, M.J. Allen, Y. Yang, R.B. Kaner, High throughput solution processing of large-scale graphene, Nat. Nanotechnol. 4 (2009) 25–29.
[18] S.J. Wang, Y. Geng, Q. Zheng, J.K. Kim, Fabrication of highly conducting and transparent graphene films, Carbon 48 (2010) 1815–1823.
[19] H.A. Becerril, R.M. Stoltenberg, M.L. Tang, M.E. Roberts, Z. Liu, Y. Chen, D.H. Kim, B.L. Lee, S. Lee, Z. Bao, Fabrication and evaluation of solution-processed reduced graphene oxide electrodes for p- and n-channel bottom-contact organic thin-film transistors, ACS Nano 4 (2010) 6343–6352.
[20] R. Karthick, M. Brindha, M. Selvaraj, S. Ramu, Stable colloidal dispersion of functionalized reduced graphene oxide in aqueous medium for transparent conductive film, J. Colloid. Interf. Sci. 5 (406) (2013) 69–74.
[21] I.Y.Y. Bu, Highly conductive and transparent reduced graphene oxide/aluminium doped zinc oxide nanocomposite for the next generation solar cell applications, Opt. Mater. 36 (2013) 299–303.
[22] E. Gyorgy, A.P.d. Pino, C. Logofatu, A. Duta, L. Isac, Effect of nitrogen doping on wetting and photoactive properties of laser processed zinc oxide-graphene oxide nanocomposite layers, Jpn. J. Appl. Phys. 116 (2014) 024906.
[23] Y. Xu, H. Bai, G. Lu, C. Li, G. Shi, Flexible graphene films via the filtration of water-soluble noncovalent functionalized graphene sheets, J. Am. Chem. Soc. 130 (2008) 5856–5857.
[24] S. Cho, J.W. Jang, J.S. Lee, K.H. Lee, Carbon-doped ZnO nanostructures synthesized using vitamin C for visible light photocatalysis, CrystEngComm 3929–3935 (2010).
[25] H. Pan, J.B. Yi, L. Shen, R.Q. Wu, J.H. Yang, J.Y. Lin, Y.P. Feng, J. Ding, L.H. Van, J.H. Yin, Room-temperature ferromagnetism in carbon-doped ZnO, Phys. Rev. Lett. 99 (2007) 127201.
[26] X.J. Ye, C.S. Liu, W. Zhong, H.A. Song, C.T. Au, Y.W. Du, Experimental and theoretical studies on the magnetic property of carbon-doped ZnO, Phy. Lett. A 374 (2010) 496–500.
[27] Z. Zhan, L. Zheng, Y. Pan, G. Sun, L. Li, Self-powered, visible-light photodetector based on thermally reduced graphene oxide–ZnO (rGO–ZnO) hybrid nanostructure, J. Mater. Chem. 22 (2012) 2589–2595.
[28] A.R. Marlinda, N.M. Huang, M.R. Muhamad, M.N. An'amt, B.Y.S. Chang, N. Yusoff, I. Harrison, H.N. Lim, C.H. Chia, S. Vijay Kumar, Highly efficient preparation of ZnO nanorods decorated reduced graphene oxide nanocomposites, Mat. Lett. 80 (2012) 9–12.
[29] X.Y. Li, H.J. Li, Z.J. Wang, H. Xia, Z.Y. Xiong, J.X. Wang, B.C. Yang, Effect of substrate temperature on the structural and optical properties of ZnO and Al-doped ZnO thin films prepared by dc magnetron sputtering, Opt. Commun. 282 (2009) 247–252.
[30] R.R. Nair, P. Blake, A.N. Grigorenko, K.S. Novoselov, T.J. Booth, T. Stauber, N.M.R. Peres, A.K. Geim, Fine structure constant defines visual transparency of graphene, Sci. 6 (2008) 1308.
[31] A.V. Moholkar, S.M. Pawar, K.Y. Rajpure, C.H. Bhosale, J.H. Kim, Effect of fluorine doping on highly transparent conductive spray deposited nanocrystalline tin oxide thin films, Appl. Surf. Sci. 255 (2009) 9358–9364.
[32] V. Khranovskyy, J. Eriksson, A. Lloyd-Spetz, R. Yakimova, L. Hultman, Effect of oxygen exposure on the electrical conductivity and gas sensitivity of nanostructured ZnO films, Thin Solid Films 517 (2009) 2073–2078.